D/H and D/O in the Galactic Disk towards the CSPN RX J2117.1+3412

Jeffrey W. Kruk and Cristina Oliveira (Johns Hopkins University)

Introduction

FUSE spectra spanning 912Å - 1187Å have been obtained for the star RX J2117.1+3412. This star is in the Galactic disk (l=80°, b=-10°) at a distance well beyond the Local Bubble: D= 760 ± 230 pc (Vauclair et al. 2002). The available measurements of D/H vary enormously at such intermediate distances, for reasons that are not yet entirely understood. It has been proposed by Linsky et al.(2006, ApJ submitted) that depletion of deuterium onto dust grains is responsible for these variations. This hypothesis appears consistent with the available data, but detailed analyses of many more sightlines, probing a variety of environments, are needed to test the hypothesis further. Whether or not this hypothesis is confirmed, additional data are required to obtain a better quantitative understanding of the evolution of D/H in the Galaxy.

RX J2117.1+3412 is a PG 1159-type central star of a planetary nebula. The stellar parameters have been determined by Werner et al. (2004). It is extremely hot: $T_{eff} = 170,000$K, with a surface gravity of $\log g = 6.00$ and an atmospheric composition of He (38%), C (54%), O (6%), and Ne (2%) (abundances by mass fraction). As a consequence of the high temperature and gravity, the photospheric features are broad and easily distinguished from the interstellar absorption features.

The *FUSE* instrument consists of 4 coaligned telescopes and spectrographs; two channels contain Al/LiF–coated optics and two contain SiC–coated optics. The LiF channels cover the wavelength range 980–1187Å, and the SiC channels span 905–1102Å. The typical spectral resolution is 0.05Å, or ∼ 15 km/s. More information about *FUSE* can be found in Moos et al. (2000) and Sahnow et al. (2000). Observations by *FUSE* were obtained through both the LWRS and MDRS apertures, as summarized in Table 1, though only the MDRS data are described here. The individual exposures were processed using version 3.1.3 of the CALFUSE pipeline, coaligned on interstellar absorption features and combined.

The *IUE* spectra were processed and combined as described in Holberg et al. (1998). The combined spectrum was downloaded from the archive at http://vega.lpl.arizona.edu/newsips/. A portion of the resulting spectrum is shown in the section below in Figure 1.

Table 1. Observation Log

Obs ID	Aperture	T_{exp}(s)	Date
D1800201	MDRS	6421	2003-06-21
D1800202	MDRS	10746	2003-06-22
P1320501	LWRS	8232	2000-07-16
SWP 47566	L	21600	1993-04-27
SWP 47563	L	21720	1993-04-28
SWP 55411	L	26400	1995-08-03

Hydrogen

The column density of neutral hydrogen was determined by fitting the damping wings of the Lyman-α profile. The *IUE* Lyman-α spectrum is shown in Figure 1. The stellar model (kindly provided by K. Werner) is plotted in green, and shows that the stellar He II absorption should have little or no impact on the interstellar H I absorption profile. The overall fit is plotted in red. There is no evidence for a wind in N V. The derived column density is $\log N_{HI}$=20.54±0.04. The uncertainty in $\log N_{HI}$is dominated by the uncertainty in the background level, and is tentative. Further work is planned to improve upon this. The Lyman edge (not shown), is well-modelled with a b-value for H I of 10.8 km s^{-1}.

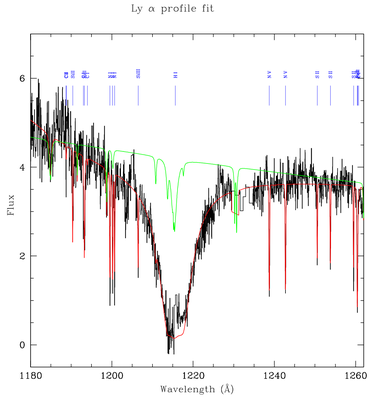

Figure 1. The H I Lyman α profile measured by *IUE* is shown. Interstellar absorption lines are labelled in blue. The overall fit is plotted in red; the green curve is the stellar model used to normalize the data in the course of the fit. The small peak at 1205Å and the sparse region at 1230Å are pixels flagged as bad, and were excluded from the fit. The geocoronal emission filling in the bottom of the IS absorption profile was also excluded from the fit.

Deuterium

The D I absorption profiles are well-separated from the the narrow H I profiles. Five of these transitions are free (or almost free) of blending with O I and H_2; these are shown in Figure 2. The 916.179Å, 920.713Å, and 925.974Å lines are uncontaminated; the 919.101Å and 937.548Å lines have modest contamination by H_2 that can be corrected with reasonable accuracy. The remaining D I lines are either significantly contaminated or saturated.

The D I transitions were analyzed by profile fitting and by a curve of growth analysis. The profile fitting was tried with both one and two velocity components; no significant second component was found. The profile fit is shown in Figure 2, and the resulting column density is $\log N_{DI}$= 15.76 ± 0.02. The curve of growth analysis, shown in Figure 3, gives $\log N_{DI}$= 15.76 ± 0.01. The uncertainties are dominated by systematics, and are still tentative.

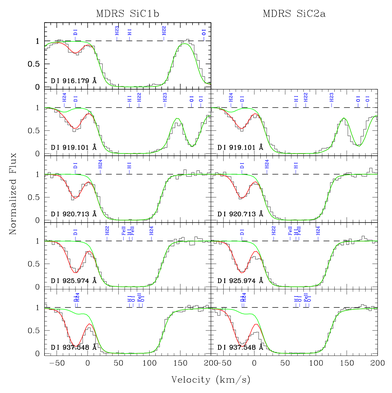

Figure 2. The most useful D I transitions are plotted as a function of velocity. The individual absorption components are labelled in blue. The overall fit is plotted in red; the green curve is the fit with N(D I)=0 to show the strength of contaminating features.

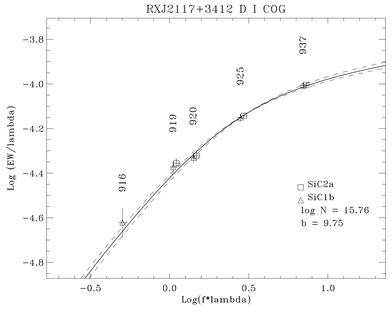

Figure 3. The equivalent widths for the D I absorption features are plotted as a function of log $f\lambda$; the best-fit curve of growth (solid line) gives $\log N_{DI}$= 15.76 ± 0.01. The dashed lines correspond to the 2σ extremes in N and b.

Oxygen

Absorption lines of O I have been analyzed by profile fitting and by curve-of growth. Numerous lines are present in the *FUSE* bandpass, with oscillator strengths that vary by a factor of 1000. However, both the profile fit and COG analyses indicate that only the weakest line (O I 974.070Å) is unsaturated. This line is shown in Figure 4. The profile fits indicate the presence of a weak second component, offset in velocity by +16km s^{-1}, that has a column density of about 1% that of the main component. An example of this second component can be seen in the red wing of the O I 1039.2306Å line shown in Figure 5. The column density determined from the profile fits is $\log N_{OI}$= 17.33±0.05; (the uncertainties at present are large because a number of systematic effects are still under investigation).

The curve of growth analysis, shown in Figure 6, gives $\log N_{OI}$= 17.31 ± 0.06. This shows that only the 974.070Å transition is clearly on the linear part of the COG. Direct integration of the two 974.070Å line profiles gives $\log N_{OI}$= 17.28 ± 0.03. All three approaches yield consistent results; the COG values will be adopted for present purposes.

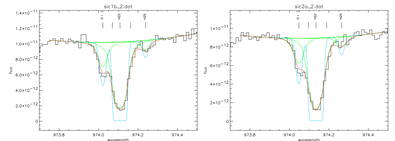

Figure 4. The SiC1 and SiC2 spectra in the vicinity of the O I 974.070Å lines are plotted. The blue curves are the intrinsic interstellar absorption profiles computed by the profile fit, the green curves are the individual components after convolution with the instrumental LSF, and the red curves are the final profile fit. The fit to the adjacent H_2 J=2 line is constrained by a simultaneous fit to all the other H_2 J=2 lines in the spectrum.

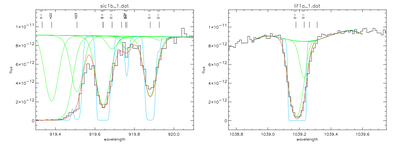

Figure 5. The left panel shows the SiC1 spectrum of the O I lines at 919.966Å and 919.917Å. The latter is the second-weakest line in the *FUSE* bandpass, but is already saturated. The right panel shows the strong line at 1039.2306Å. The weak second velocity component is clearly seen on the red wing of the line profile.

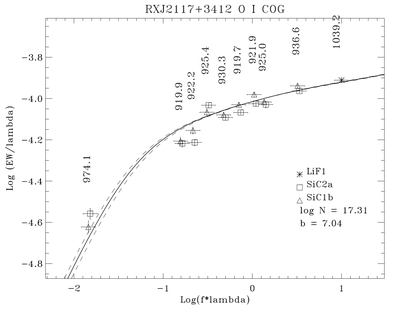

Figure 6. The equivalent widths for the O I absorption features are plotted; the best-fit curve of growth (solid line) gives $\log N_{OI}$= 17.31 ± 0.06 and b = 7.04km s^{-1}.

Nitrogen

The profile fit to the N I lines yields $\log N_{NI}$= 16.35 ± 0.03. A sample of the profile fits is shown in Figure 7.

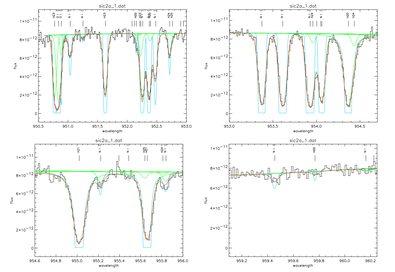

Figure 7. The most useful N I transitions are plotted as a function of wavelength. The blue curve is the model before convolution with the instrument LSF; the red curve after convolution.

Molecular Hydrogen

Molecular hydrogen is observed at velocity 2-3 km s^{-1} to the blue of the atomic gas, and is detected for J = 0 – 5. The J=0,1 transitions exhibit damped profiles and the J=4,5 transitions are quite weak, so the column densities for J-levels can be measured reliably. The J=2-3 transitions, however, are on the flat part of the curve of growth except for the weakest transitions, so their column densities are not as accurate. Figure 8 shows a sample of H_2 lines, and the column densities are listed in Table 2. The log of the total H_2 column density is log N = 18.76, giving a molecular fraction of 0.0165.

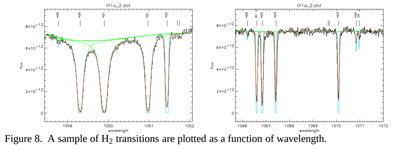

Figure 8. A sample of H_2 transitions are plotted as a function of wavelength.

Table 2. H_2Column Densities

J	0	1	2	3	4	5	HD(J=0)
Log N	18.24	18.60	16.22	15.72	14.06	13.47	13.41

Iron

The numerous Fe II transitions in the *FUSE* bandpass have been analyzed in the same manner as O I. The column density derived from the COG fit is $\log N_{FeII}= 14.60^{+0.01}_{-0.02}$. As can be seen from the plot in Figure 9, the uncertainty in logN is dominated by apparent discrepancies in the f-values. The result from the profile fit is $\log N_{FeII}$= 14.58; the uncertainty will be evaluated after further investigation of the f-values.

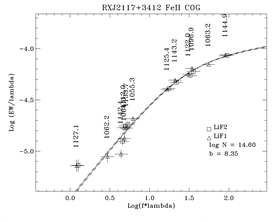

Figure 9. The curve of growth analysis for Fe II is shown. The scatter about the fit is dominated by uncertainties in the f-values for the transitions.

Results

Table 3 Measured Column Densities & Abundance Ratios

Column Density		Abundance Ratio (ppm)		
Species	Log N	Ratio	FUSE	Solar
H I	20.54±0.04	…	…	…
D I	15.76±0.02	D I/H I	16.60±1.7	15.6
O I	17.31±0.06	O I/H I	588.8±98	458
N I	16.53±0.03	N I/H I	64.6±7.4	85.1
Fe II	14.60±0.02	Fe II/H I	1.15±0.12	31.6

The H I column density of $\log N_{HI}$=20.54 places this line of sight at the upper end of the so-called "intermediate column density regime," ($\log N_{HI}$of 19.2–20.7), for which D/H ranges from 5 to 23ppm. It is thought that, for these column densities, the line of sight extends well beyond the local bubble, but not so far that one averages over many different environments. Thus the range of observed D/H values reflect the range of processes that can affect the state of IS gas on moderate size scales. Five of the available 17 measurements have D/H values >19ppm, but the remainder are all below 13ppm. The value D/H for this sightline, 16.6±1.7 ppm, is relatively high and thus helps to further define the boundary between the intermediate and high column density regimes. All 5 of the measurements available at higher column densities have D/H ≤ 10ppm.

The value for O/H is 589 ± 98 ppm, just barely consistent with the solar abundance of 458±53 ppm (Asplund et al. 2004). This is, however, considerably higher than the typical gas-phase abundance of 343 ppm found by Meyer et al. (1998) or 408 ppm found by André et al. (2003). The total oxygen abundance was estimated by Meyer et al. (1998) to be 520 ppm after allowing for depletion, roughly matching the solar value. This implies that little, if any, oxygen is bound in dust along this sightline.

The value for D/O of $2.82 \pm 0.41 \times 10^{-2}$ is significantly below the typical LISM value of 3.84×10^{-2} (Hébrard and Moos 2003), but is not atypical for lines of sight with $\log N_{HI} > 20.3$.

The N I abundance is quite close to the solar value (Holweger 2001). The N II lines available are highly saturated, so they cannot be used to determine ionization corrections to the N abundance. The N I abundance is thus a lower limit for the total abundance of N.

The Fe II gas-phase abundance is depleted by 1.44 dex relative to solar, slightly more than is typical for the warm disk gas. This is consistent with the modest extinction along this line of sight, E(B-V)=0.05, which in turn is in good agreement with what is expected for typical disk sightlines (E(B-V) = N(H)/5.8 · 10^{21}) (Bohlin et al. 1978)). Similarly, the molecular fraction (0.0165) is typical of warm disk gas.

The results of the preliminary analysis presented here are generally consistent with the time-varying depletion model proposed by Linsky *et al.*(2006), in which the abundance of D is modulated by preferential depletion onto dust grains. Further work is planned to refine these measurements and to obtain information on other consituents of the gas along the line of sight.

The profile fitting was performed using the program "Owens" written by Martin Lemoine. The NASA-CNES-CSA *FUSE* mission is operated by the Johns Hopkins University. Financial support to U. S. participants has been provided by NASA contract NAS5-32985.

REFERENCES

André, M. K., et al. 2003, ApJ, 591, 1000.

Asplund, M., Grevesse, N., Sauval, A. J., Allende Prieto, C., & Kiselman, D. 2004, A&A, 417, 751.

Bohlin, R. C., Savage, B. D., & Drake, J. F. 1978, ApJ, 224, 132.

Hébrard, G., & Moos, H. W. 2003, ApJ, 599, 297.

Holberg, J. B., Barstow, M. A., & Sion, E. M. 1998, ApJS, 119, 207.

Holweger, H. 2001. In *AIP Conf. Proc. 598: Joint SOHO/ACE workshop "Solar and Galactic Composition"*, pp. 23.

Meyer, D. M., Jura, M., & Cardelli, J. A. 1998, ApJ, 493, 222.

Moos, H. W., et al. 2000, ApJ, 538, L1.

Sahnow, D. J., et al. 2000, ApJ, 538, L7.

Vauclair, G., et al. 2002, A&A, 381, 122.

Werner, K., Rauch, T., Reiff, E., Kruk, J. W., & Napiwotzki, R. 2004, A&A, 427, 685.

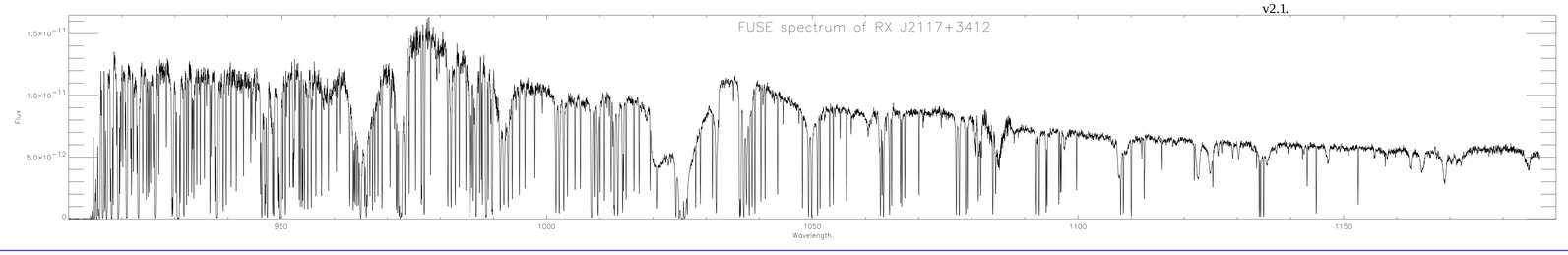

This poster was prepared with Brian Wolven's Poster LaTeX macros v2.1.

Table 1:

Table 2:

Fig. 1.—

Fig. 2.—

Fig. 3.—

Fig. 4.—

Fig. 5.—

Fig. 6.—

Fig. 7.—

Fig. 8.—

Fig. 9.—

Table 3: